Development of A Resonant Excitation Coil of AC Magnetometer for Evaluation of Magnetic Fluid

Mohd Mawardi Saari[1], Nazatul Sharreena Suhaimi[1], Saifudin Razali[1], Nurul Akmal Che Lah[2], Kenji Sakai[3], Toshihiko Kiwa[3] and Keiji Tsukada[3]
[1]*Faculty of Electrical & Electronic Engineering, Universiti Malaysia Pahang, 26600 Pekan, Pahang, Malaysia*
[2]*Innovative Manufacturing, Mechatronics and Sports Lab (iMAMS), Faculty of Manufacturing Engineering, Universiti Malaysia Pahang, 26600 Pekan, Pahang, Malaysia*
[3]*Graduate School of Natural Science and Technology, Okayama University, 3-1-1 Tsushima Naka, 700-8350 Okayama, Japan*
mmawardi@ump.edu.my

***Abstract*—A high-homogeneity excitation coil with a resonant circuit for AC magnetometer is developed. A solenoid coil is designed to produce a high-homogeneity and strong excitation field using a resonant frequency method. The solenoid coil is fabricated with a Litz wire to suppress the increase of AC resistance due to the skin and proximity effects in the high-frequency region. The Litz wire is composed of 60 strands of copper wires with 0.1-mm diameter. The resonant frequency method is applied to cancel the reactance component by connecting the excitation coil with a capacitor in a series configuration. To enable excitation of the magnetic field at multiple frequencies, a resonant circuit consists of multiple values of resonant capacitors is constructed. The fabricated excitation coil showed a high homogeneity of the magnetic field and was able to maintain a constant resonant current up to 32.5 kHz.**

***Index Terms*—Coil; Impedance; Magnetometer; Resonant Circuit.**

I. INTRODUCTION

Magnetic nanoparticles (MNPs) are commonly applied in biomedical such as *in vivo*-imaging, magnetic hyperthermia and magnetic immunoassay [1], [2]. Their characteristics of magnetic properties are being utilized in different applications of magnetic nanoparticles where these applications require distinct features of MNPs. Due to this reason, the characterization of the magnetic nanoparticles is important so that they can be optimized for the intended applications. The magnetic properties of the magnetic nanoparticles can be characterized using magnetic susceptibility [3], [4], relaxation [5]–[7] and remanence measurements [8], [9]. AC susceptibility method is commonly utilized because it can provide information on size distribution, harmonics, magnetic anisotropy, relaxation etc. with a fast response to the measurement [10]. However, there are some technical issues need to be solved in this method such as sensitivity reduction due to the interference of excitation magnetic field, inhomogeneity of excitation magnetic field, the limited magnitude of excitation magnetic field at high frequencies and so on [11], [12].

In order to achieve high homogeneity and sufficient magnitude of excitation magnetic field in high-frequency regions, an excitation coil with a resonant circuit is developed in this work. The excitation coil is constructed from two solenoid coils which are connected in series and separated by 4 mm of distance. The excitation coil is designed so that a strong and uniform magnetic field can be generated at its axis while maintaining a compact size. Furthermore, the distribution of magnetic field is simulated during optimization of the radius and length of the excitation coil.

The excitation magnetic field is generated based on Biot-Savart's law where a current is supplied to the excitation coil by a power supply. For evaluation of AC susceptibility value of MNPs, an AC excitation magnetic field is applied to MNPs, and their AC response is measured. However, in the case of operating the excitation coil at a high frequency, the coil's impedance will increase significantly due to its inductance as well as the AC resistance. The utilization of Litz wire in the construction of the excitation coil can reduce the AC resistance [13], [14], however, reduction of coil's inductance will decrease the strength of the excitation magnetic field as it relates to the number of turns. Although using a superior power supply can overcome this issue, it is an expensive solution. On the other hand, the reactance of the excitation coil can be simply reduced by using capacitors to form a resonant RCL circuit with the expense of a narrow-band excitation frequency [15], [16]. To achieve a broad resonant frequency of up to 82.32 kHz, a resonant circuit consists of multiple resonant capacitors is developed in this work.

II. METHODOLOGY

A. System Configuration

Figure 1 shows a schematic diagram of the developed AC magnetometer system. The developed system consists of inductive excitation and detection coils. The excitation coil is connected to a current amplifier (TS 250, Accel Instruments). A lock-in amplifier (LI 5640, NF Corporation) is used for the signal detection of the inductive detection coil. Based on the reference signal from the lock-in amplifier, it will act as a function generator and provide a sine wave signal to the current amplifier. The current amplifier converts the signal to a high current signal and supplies it to the excitation coil. The excitation field will magnetize a sample that is placed inside the excitation coil. Subsequently, the magnetization of the sample produces a magnetic field where the detection coil will detect this magnetic field. The lock-in detected signal of the detection coil is sent to a computer for signal analysis.

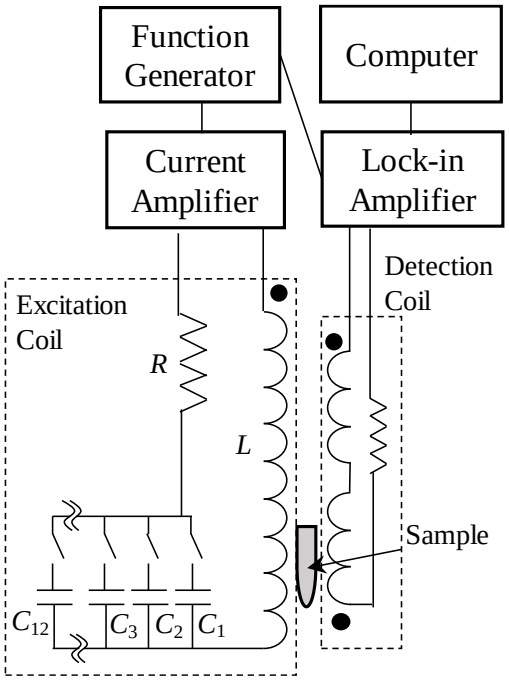

Figure 1: Schematic diagram of the developed system.

B. Development of The Excitation Coil

The design of the excitation coil is optimized by analyzing the internal distribution of the magnetic field. In this work, the Biot-Savart's equation based on a multi-layer surface current model was used in the simulation of the magnetic field distribution. The magnetic field **B(r')** at observation point **r'** resulted from multi-layer surface current can be expressed as:

$$\mathbf{B}(\mathbf{r}') = \frac{\mu_0}{4\pi}\sum_{n=1}^{N}\sum_{i=1}^{S}\frac{\mathbf{J}_n s_{i,n}\times(\mathbf{r}'-\mathbf{r}_n)}{\left|\mathbf{r}'-\mathbf{r}_n\right|^3}, \qquad (1)$$

where μ_0 is the vacuum magnetic permeability, $\mathbf{J}_n$ is the surface current density vector at n layer, $s_{i,n}$ is the unit area of the surface S and $\mathbf{r}_n$ is the position of the surface current. From Equation (1), it is evident that reducing the distance between current element $\mathbf{r}_n$ and point observation **r'** can result to increase in the magnetic field. This is equal to the reduction in the radius of the excitation coil. However, if the radius is too small, this will reduce the uniform area of the magnetic field; therefore, an optimum radius must be selected where the size of the sample and detection coil are also being considered. It should be noted that the intensity of the magnetic field can be increased by increasing the number of layer n. However, this will result to increase in resistance and inductance. Furthermore, impedance increase due to proximity effect and core losses can be expected when n is too high. Therefore, a moderate value of a number of n must be considered. From the numerical simulations of the magnetic field distribution, the excitation coil was fabricated of two identical solenoid coils which were connected in series. A 4-mm gap was placed between the solenoid coils for cooling purpose. The number of turn for one solenoid coil was 150 turns and was fabricated with the Litz wire. The Litz wire was composed of 60 strands of copper wires with 0.1-mm diameter. The radius and length of one solenoid coil were 15 mm and 26 mm. The resistance and inductance of the excitation coil were measured to be 1.3516 Ω and 1.5176 mH at 1 V and 1 kHz.

C. Resonant Circuit

When the excitation coil is connected to the power supply, the electrical circuit is equal to an *RL* circuit where self-capacitance of the excitation coil is small and can be ignored [17]. The impedance of the *RL* circuit can be expressed as:

$$Z(\omega) = R_{DC} + R_{AC}(\omega) + j\omega L, \qquad (2)$$

where $\omega = 2\pi f$ is angular frequency, R_{DC} is the DC resistance, R_{AC} is AC resistance, and L is the inductance of the excitation coil. Here, R_{DC} is constant while R_{AC} is a function of ω. From Equation (2), the impedance increases with respect to the frequency where a 10^3-fold increase in frequency will result in a 10^3-fold increase in the impedance. This means that to maintain a constant flow of current, the supply voltage must be increased by 10^3 times. When a capacitor C is connected to the excitation coil, the equivalent electrical circuit can be expressed as:

$$Z(\omega) = R_{DC} + R_{AC}(\omega) + j(\omega L - 1/\omega C). \qquad (3)$$

When the circuit turns into a resonant mode where the imaginary part of the impedance becomes zero, the resonant frequency f_R can be expressed as:

$$f_R = \frac{1}{2\pi\sqrt{LC}}. \qquad (4)$$

In this mode, the flowing current is limited by the resistance of the circuit only and a clean sine wave current can be obtained as the circuit acts as a band-pass filter. Moreover, the resonant frequency can be selected by using different values of C.

Based on these designs, a resonant circuit composed of multiple values of polypropylene film capacitors was designed and fabricated. The range of the resonant frequency was set from 581 Hz to 82.32 kHz. To achieve the desired resonant frequencies, capacitor networks consist of combinations of parallel and/or series connections were fabricated. The calculated and measured resonant frequencies were compared as well to the impedance.

III. Experimental Result

The normalized distribution of the simulated excitation magnetic field B_y and B_z is shown in Figure 2. The axis of the excitation coil was set to z = 1.7 cm. The distributions were calculated at 2-mm interval in the region of 0 mm ≤ y ≤ 90 mm and –15 mm ≤ z ≤ 15 mm. The contours were divided by 5%-interval. From the distributions of B_y and B_z, a homogeneity of 95% could be obtained when the sample was placed at a y-position of 35 mm to 55 mm. Figure 3 shows the calculated and measured distribution of excitation magnetic field B_y along the axis of the excitation coil. The distribution of magnetic field along the axis of the excitation coil was measured using a Teslameter. The strength of the excitation magnetic field per unit current at the centre was measured to be 5.2 mT/A. The simulation agreed well with the measured distribution. From the result, the magnetic field showed a high uniformity in the region of 30 mm to 60 mm and sufficient for a cylindrical sample of 10-mm diameter and

10-mm length. In this region, the inhomogeneity was calculated to be 6%.

Figure 4 shows the calculated impedance of the excitation coil when it is connected to different values of capacitors. Here, the resistance was assumed as constant over frequency. As a comparison, the impedance of the *RL* circuit is also shown. The impedance of the *RL* circuit increases rapidly

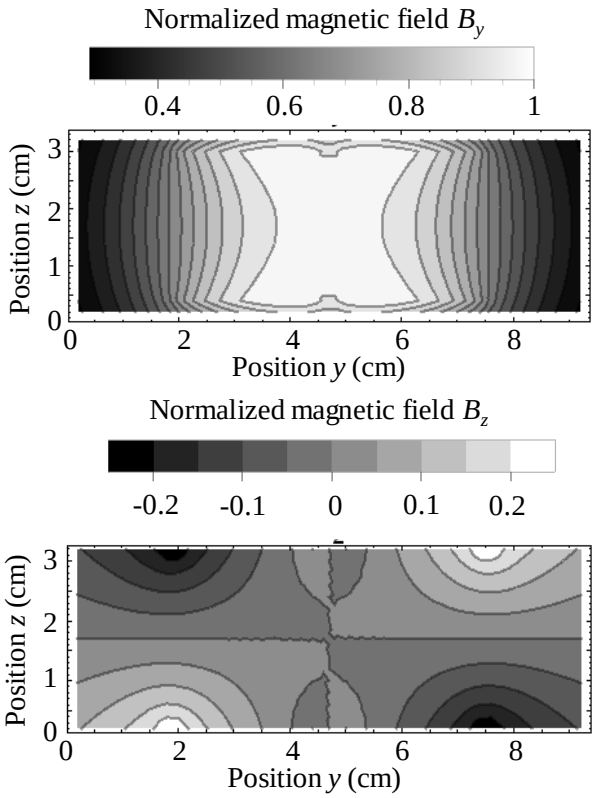

Figure 2: The distribution excitation magnetic field B_y and B_z inside the excitation coil.

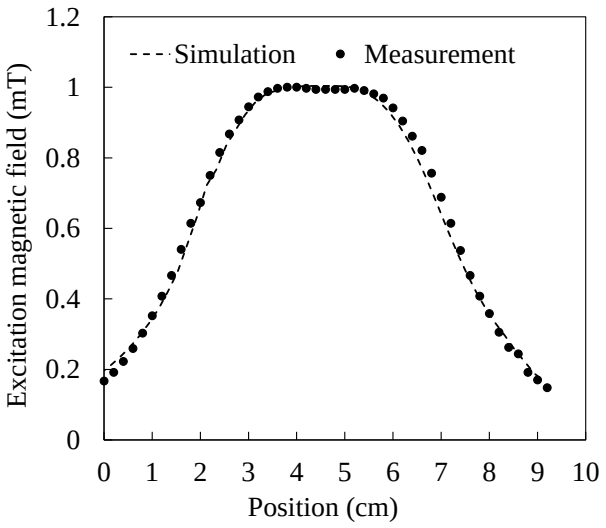

Figure 3: The distribution line of excitation magnetic field with respect to the position along the axis of the excitation coil.

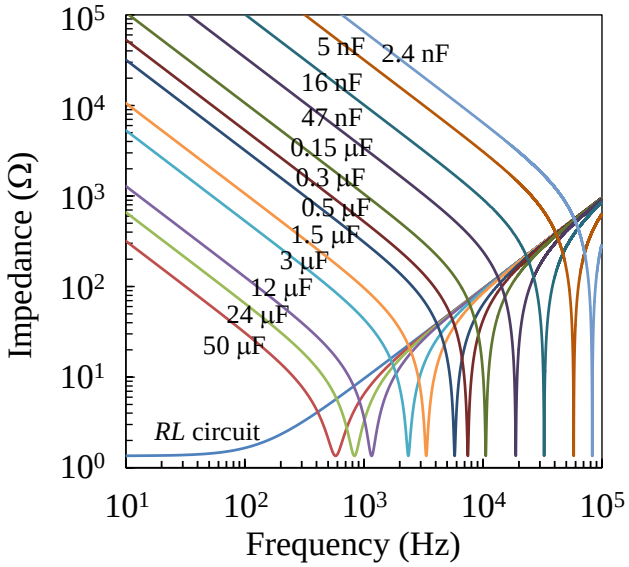

Figure 4: The impedance of the series *RCL* circuit.

when the frequency is larger than 100 Hz. When the *RL* circuit is connected to capacitors, the impedance due to the capacitance is dominance in the region below the resonant frequency. The impedance reaches a minimum value when the circuit is at resonance. As the frequency becomes larger than the resonant frequency, the impedance increases due to inductance. As shown in Fig. 4, the impedance demonstrated a characteristic of a narrow-band filter where a maximum current can be obtained at the resonant frequency.

The calculated and measured resonant frequencies are shown in Figure 5. The resonant frequency was determined by measuring the flowing current to the excitation coil while sweeping the frequency of power supply in constant voltage mode. The resonant frequency was determined when the flowing current reached a maximum value. From Figure 5, it can be shown that the measured resonant frequency agreed to the calculated frequency. The measured resonant frequency was slightly larger compared to the calculated resonant frequency. This could result in slight differences of capacitance in the fabricated capacitor networks.

The measured current of the *RCL* circuit in resonance mode at different capacitor values is shown in Figure 6. The current was measured when the power supply was operated in the constant voltage mode. The magnitude of the current could be maintained without significant decrease until 32.5 kHz when the excitation coil was operated in the resonance mode. In the region higher than 10 kHz, a rapid decrease of current's magnitude was observed, and this might be caused by the significant increase in resistance and core losses. As a comparison, the flowing current of the *RL* circuit was also shown in Figure 6. The flowing current decreased inverse-proportionally with the frequency. The current in the *RL* circuit was reduced by 100 times at 32.5 kHz compared to the *RCL* circuit in the resonance mode. From this, it can be shown that the benefit of the resonant circuit to drive the excitation coil at high frequency.

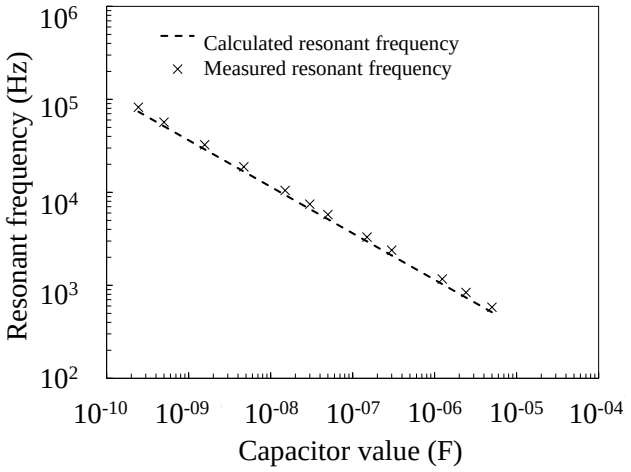

Figure 5: Resonant frequency of series *RCL* circuit with respect to capacitor values.

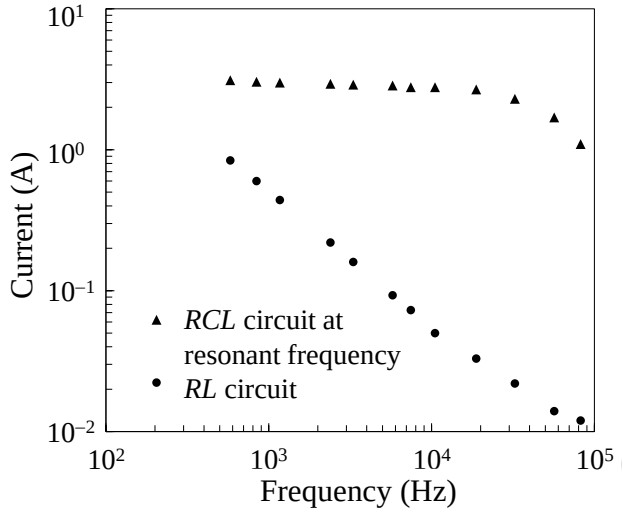

Figure 6: The current at the excitation coil when the power supply was operated in the constant voltage mode.

IV. CONCLUSION

A high-homogeneity of excitation coil with a resonant circuit for AC magnetometer has been developed for evaluation of the magnetic response of the MNPs. The excitation coil was fabricated from a Litz wire to reduce AC resistance at high frequency. The fabricated excitation coil showed a non-uniformity of 6% within a 30-mm region, which was sufficient for the size of a 1-mL sample. A resonant circuit consists of multiple capacitor values was designed and fabricated. The magnitude of the flowing current from the power supply was successfully maintained until 32.5 kHz when the excitation coil was operated in the resonance mode. Improvement of the current at a higher frequency can be expected by taking into consideration of coil's AC resistance and core losses during the design of the excitation coil. It is expected that the developed excitation coil system can be utilized for harmonics and magnetic relaxation measurement of MNPs.

ACKNOWLEDGMENT

This work was supported by Ministry of Higher Education of Malaysia under grant number of RDU 160115 and Research Management Center of Universiti Malaysia Pahang under grant number of RDU 170377.

REFERENCES

[1] M. M. Saari, K. Sakai, T. Kiwa, T. Sasayama, T. Yoshida, and K. Tsukada, "Characterization of the magnetic moment distribution in low-concentration solutions of iron oxide nanoparticles by a high-Tc superconducting quantum interference device magnetometer," *J. Appl. Phys.*, vol. 117, no. 17, p. 17B321, May 2015.

[2] Y. Higuchi, S. Uchida, A. K. Bhuiya, T. Yoshida, and K. Enpuku, "Characterization of Magnetic Markers for Liquid-Phase Detection of Biological Targets," *IEEE Trans. Magn.*, vol. 49, no. 7, pp. 3456–3459, Jul. 2013.

[3] [K. Enpuku, T. Tanaka, Y. Tamai, and M. Matsuo, "AC susceptibility of magnetic markers in suspension for liquid phase immunoassay," *J. Magn. Magn. Mater.*, vol. 321, no. 10, pp. 1621–1624, May 2009.

[4] F. Ahrentorp *et al.*, "Sensitive high frequency AC susceptometry in magnetic nanoparticle applications," *AIP Conf. Proc.*, vol. 1311, no. 2010, pp. 213–223, 2010.

[5] A. Guillaume, J. M. Scholtyssek, A. Lak, A. Kassner, F. Ludwig, and M. Schilling, "Magnetorelaxometry of few Fe3O4 nanoparticles at 77K employing a self-compensated SQUID magnetometer," *J. Magn. Magn. Mater.*, vol. 408, pp. 46–50, 2016.

[6] F. Ludwig, E. Heim, S. Mäuselein, D. Eberbeck, and M. Schilling, "Magnetorelaxometry of magnetic nanoparticles with fluxgate magnetometers for the analysis of biological targets," *J. Magn. Magn. Mater.*, vol. 293, no. 1, pp. 690–695, May 2005.

[7] H. C. Bryant *et al.*, "Magnetic Properties of Nanoparticles Useful for SQUID Relaxometry in Biomedical Applications.," *J. Magn. Magn. Mater.*, vol. 323, no. 6, pp. 767–774, Mar. 2011.

[8] A. Tsukamoto *et al.*, "Improvement of sensitivity of multisample biological immunoassay system using HTS SQUID and magnetic nanoparticles," *Phys. C Supercond.*, vol. 445–448, pp. 975–978, Oct. 2006.

[9] A. Tsukamoto *et al.*, "Reduction of the magnetic signal from unbound magnetic markers for magnetic immunoassay without bound/free separation," *Phys. C Supercond.*, vol. 463–465, pp. 1024–1028, Oct. 2007.

[10] A. Prieto Astalan *et al.*, "Magnetic response of thermally blocked magnetic nanoparticles in a pulsed magnetic field," *J. Magn. Magn. Mater.*, vol. 311, no. 1 SPEC. ISS., pp. 166–170, 2007.

[11] P. Baranov, V. Baranova, S. Uchaikin, and Y. Pisarenko, "Creating a uniform magnetic field using axial coils system for calibration of magnetometers," pp. 0–4, 2010.

[12] M. M. Saari *et al.*, "Optimization of an AC/DC High-Tc SQUID Magnetometer Detection Unit for Evaluation of Magnetic Nanoparticles in Solution," *IEEE Trans. Appl. Supercond.*, vol. 25, no. 3, pp. 1–4, Jun. 2015.

[13] K. Enpuku *et al.*, "Performance of Pickup Coil Made of Litz Wire and Coupled to HTS SQUID," *Phys. Procedia*, vol. 36, pp. 400–404, Jan. 2012.

[14] V. Connord, B. Mehdaoui, R. P. Tan, J. Carrey, and M. Respaud, "An air-cooled Litz wire coil for measuring the high frequency hysteresis loops of magnetic samples - A useful setup for magnetic hyperthermia applications," *Rev. Sci. Instrum.*, vol. 85, no. 9, 2014.

[15] P. W. Goodwill, G. C. Scott, P. P. Stang, and S. M. Conolly, "Narrowband magnetic particle imaging.," *IEEE Trans. Med. Imaging*, vol. 28, no. 8, pp. 1231–7, Aug. 2009.

[16] K. Enpuku, S. Hirakawa, R. Momotomi, M. Matsuo, and T. Yoshida, "Performance of HTS SQUID using resonant coupling of cooled Cu pickup coil," *Phys. C Supercond.*, vol. 471, no. 21–22, pp. 1234–1237, Nov. 2011.

[17] T. Q. Yang and K. Enpuku, "SQUID magnetometer utilizing normal pickup coil and resonant-type coupling circuit," *Phys. C Supercond.*, vol. 392–396, pp. 1396–1400, Oct. 2003.